ISSN 0208-7774 TRIBOLOGIA 3/2019 p. 71–77
DOI: 10.5604/01.3001.0013.5436

Dmitrij MOROZOW[*], Mirosław RUCKI[**], Zbigniew SIEMIĄTKOWSKI[***], Yuriy GUTSALENKO[****]

TRIBOLOGICAL TESTS OF THE CERAMIC CUTTING TOOLS AFTER YTTRIUM (Y^+) AND RHENIUM (Re^+) ION IMPLANTATION

BADANIA TRIBOLOGICZNE CERAMICZNYCH NARZĘDZI SKRAWAJĄCYCH PO IMPLANTACJI JONAMI ITRU (Y^+) I RENU (Re^+)

Key words: ion implantation, tribological test, wear, friction, cutting tool.

Abstract The paper presents the results of investigations on the tribological properties of cutting tools after ion implantation. The research focused on the inserts made out of nitride ceramics IS9 (Si_3N_4 with additives) and combined ceramics IN22 (Al_2O_3 + TiCN) available on the market. The inserts rake surfaces were covered with yttrium and rhenium coatings by means of ion implantation with different dozes. Both unimplanted and coated surfaces underwent tribological tests of the block-on ring type. The experiments demonstrated that, in general, ion implantation with rhenium (Re^+) and yttrium (Y^+) provided a decrease in surface friction forces. In the case of IN22 ceramics, both rhenium and yttrium ions improved wear resistance of cutting inserts. On the other hand, Re^+ implantation provided the best wear resistance of the IS9 ceramics.

Słowa kluczowe: implantacja jonów, test tribologiczny, zużycie, tarcie, narzędzie skrawające.

Streszczenie Artykuł opisuje wyniki badań właściwości tribologicznych narzędzi skrawających po implantacji jonów. Badania dotyczyły narzędzi wykonanych z ceramiki azotkowej IS9 (Si_3N_4 + dodatki) i ceramiki mieszanej IN22 (Al_2O_3 + TiCN), dostępnych na rynku. Na powierzchnie natarcia naniesiono powłoki itru i renu metodą implantacji jonów o różnych dawkach. Pokryte i niepokryte powierzchnie zostały poddane testom tribologicznym w parach typu rolka–klocek. Badania wykazały, że generalnie implantacja jonów renu (Re^+) i itru (Y^+) zmniejsza siły tarcia na powierzchni. W przypadku ceramiki IN22 iony zarówno renu, jak i itru zwiększyły odporność płytek skrawających na zużycie. Z drugiej strony, najlepszą odporność na zużycie ceramiki IS9 zapewniły jony renu.

INTRODUCTION

The wear conditions of different cutting tools have a huge effect on production cost, energy consumption, and carbon emission, so they should not be ignored **[L. 1]**. The wear of the cutting tools depends on their tribological properties **[L. 2]**, vibration **[L. 3]**, cutting forces **[L. 4]**, cooling conditions **[L. 5]**, etc. Some reports demonstrated that almost all physico-mechanical properties of the tool material responsible for its wear resistance can be changed with the ion beam irradiation **[L. 6]**. Ion implantation effects surface contour, microhardness, micro-, and submicro-structures, as well as the chemical composition of surface layers of cermet hard alloy tools and high-speed steel tools **[L. 7]**. Ion implantation seems to be especially advantageous for the cutting tools apply to hard to machine alloys **[L. 8]**. It is stated that ca. 85% of cemented carbide tools are coated, and nanostructured PVD coatings very quickly found wide applications in this area **[L. 9]**.

[*] ORCID: 0000-0002-3963-6749. Kazimierz Pulaski University of Technology and Humanities in Radom, Faculty of Mechanical Engineering, Radom, Poland.
[**] ORCID: 0000-0001-7666-7686. Kazimierz Pulaski University of Technology and Humanities in Radom, Faculty of Mechanical Engineering, Radom, Poland.
[***] ORCID: 0000-0002-6830-4479. Kazimierz Pulaski University of Technology and Humanities in Radom, Faculty of Mechanical Engineering, Radom, Poland.
[****] ORCID: 0000-0003-4701-6504. National Technical University "Kharkiv Polytechnic Institute", Kharkiv, Ukraine.

In the previous study, yttrium ions were implanted on the surface of the cemented carbide cutting inserts with TiN coatings. Results demonstrated their improved cutting performance in terms of reduced cutting forces and wear parameters **[L. 10]**. The present study is focused on tribological properties of the ceramic cutting tool materials after yttrium and rhenium ion implantation.

MATERIALS AND METHODOLOGY

In the research, the cutting inserts type TNGA 160408E (IS9) and TNGA 160408T (IN22) produced by ISCAR were used. They were made out of nitride ceramics IS9 (Si_3N_4 with additives) and combined ceramics IN22 (Al_2O_3 + TiCN), respectively. The initial inserts are shown in **Fig. 1**.

The rake surfaces of the inserts were implanted with the ions using a TITAN device equipped with a spark source of metal vapour MEVVA type (Metal Vapour Vacuum Arc). The implantation involved ions of yttrium (Y^+) and rhenium (Re^+), and parameters of the processes are shown in **Table 1**. The implantation procedure and its assessment with scanning electron microscope EVO MA10 were performed in the Polish National Centre of Nuclear Research (NCBJ).

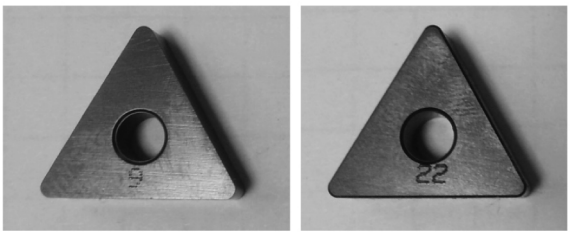

Fig. 1. Cutting inserts TNGA 160408E (IS9) and TNGA 160408T (IN22) produced by ISCAR

Rys. 1. Płytki skrawające TNGA 160408E (IS9) oraz TNGA 160408T (IN22) firmy ISCAR

Table 1. Parameters of the ceramic inserts with ion implantation

Tabela 1. Parametry implantacji płytek z ceramiki narzędziowej

No.	Insert material	Ion type	Ion doze	Energy
1	TNGA 160408E nitride ceramics IS9	Re^+	1×10^{17} ion/cm^2	65 keV
2	TNGA 160408E nitride ceramics IS9	Y^+ Y^+	1×10^{17} ion/cm^2 2×10^{17} ion/cm^2	65 keV
3	TNGA 160408T combined ceramics IN22	Re^+	1×10^{17} ion/cm^2	65 keV
4	TNGA 160408T combined ceramics IN22	Y^+ Y^+	1×10^{17} ion/cm^2 2×10^{17} ion/cm^2	65 keV

There are many methods and devices designed to evaluate tribological characteristics of PVD coatings **[L. 11]**. The increase in forces during machining has an impact on the tool life **[L. 12]**, so it was necessary to perform tests on friction forces before and after ion implantation of cutting tools. Tribological tests were performed with a T-05 device produced by Institute of Sustainable Technologies at National Research Institute in Radom **[L. 13]**. The T-05 device is a block-on ring type wear tester designed for evaluation of lubricants, engineering materials, and coatings, especially those of the highly loaded machine elements. It provides sliding or oscillating movement with a sliding velocity up to 5.5 m/s at a frequency up to 8 Hz and a normal load up to 3150 N.

The experiments were performed in the conditions required in the project VAMAS (Versailles Project on Advanced Materials and Standards) performed by the participants from G-7 countries, Poland and Finland, and in the Program COST Action 516 **[L. 14]**. Namely, there was a sliding speed of 0.1 m/s under a 10 N load. In our research, however, the load was increased up to 100 N because of high loads in the real work conditions of a cutting edge. Environmental conditions were supervised, and the experiments were made in a humidity of 50% at a temperature of 23°C.

In the tester, the roller was used made out of the bearing steel ŁH15/1.3505/100CR6 according to the standard PN-EN ISO 683-17:2015-01. The roles of fixed blocks samples simulated the inserts made out of ceramics IN22 or IS9. They were pressed with certain force *P* against the roller rotating in one direction with certain rotational speed, as shown in **Fig. 2.** The contact *S* was non-conformal (line), and the hemispherical insert ensured steady distribution of the pressure in the contact zone. A thermocouple was used to measure the temperature of the block. The friction couple was inserted in the reservoir, which enabled tests both with and without a lubricating liquid. In order to fix the examined cutting inserts in the device T-05, special adaptive holders were made, as shown in **Fig. 3**.

a) b)

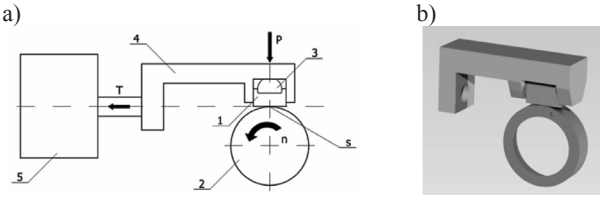

Fig. 2. The friction couple of the block-on ring type: a) scheme [L. 15], b) 3D view [L. 16], 1 – flat surface sample, 2 – roller, 3 – hemisphere insert, 4 – sample holder

Rys. 2. Skojarzenie „rolka–klocek”: a) schemat **[L. 15]**, b) model przestrzenny **[L. 16]**, 1 – klocek płaski (próbka), 2 – rolka (przeciwpróbka), 3 – wkładka półkulista, 4 – uchwyt próbki

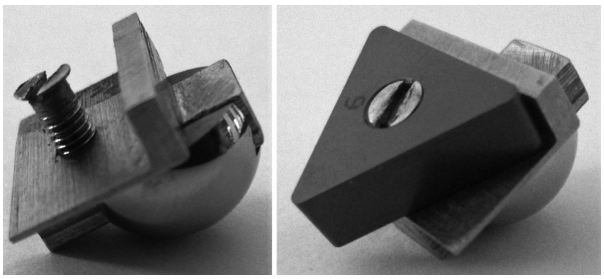

Fig. 3. Adaptive holder for triangle cutting insert tribological test

Rys. 3. Uchwyt specjalny do trójkątnych płytek skrawających

Tribological tests were performed in the following conditions:

– Rotational speed n = 56 rpm, which resulted with sliding speed ca. v = 0.1 m/s for the roller diameter D = 37 mm, according to the following equation:

$$n = 60\frac{v}{\pi D} = 60\frac{0.1}{\pi \cdot 0.037} \approx 52[\text{rpm}] \tag{1}$$

where

– pressing force P = 100 N,
– friction path S = 100 m,
– the number of cycles, i.e. rotations of the roller N = 860, according to the following equation:

$$N = \frac{S}{\pi D} = \frac{100}{\pi \cdot 0.037} \approx 860[-] \tag{2}$$

where

– testing time $t \approx 1000$ s, according to the following equation:

$$t = \frac{N}{n} = \frac{860}{52:60} \approx 1000[s] \tag{2}$$

where the lubricator was 5% water emulsion B-Cool 655 (chlorine-free semisynthetic coolant with mineral oil added) produced by Blaser Swisslube AG.

RESULTS AND DISCUSSION

After the ion implantation procedure, the rake surfaces of the inserts were checked for qualitative assessment. The maps of respective substances Y and Re were obtained with the points representing them with higher density and brightness in the areas with higher substance content. **Figure 4** shows examples of the Y and Re distribution maps on the ceramic surfaces.

In was found that the obtained distribution of coating elements was similar for both examined ceramic materials. Presence and steady distribution of ions Y^+ and Re^+ were asserted on both IN22 and IS9 cutting inserts surfaces.

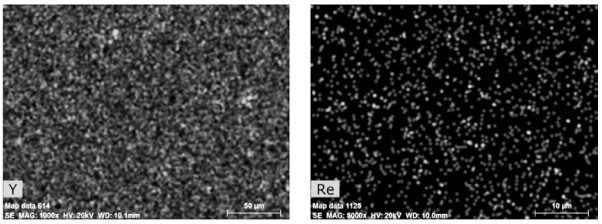

Fig. 4. Examples of the yttrium and rhenium distribution on the cutting inserts rake surfaces

Rys. 4. Przykłady rozkładu pierwiastków itru i renu na powierzchni natarcia płytek skrawających

From each tribological test, reports were generated with obtained values of friction force F_t, total linear wear d, and sample temperature T versus time t. The values d and T did not changed significantly during the tests, with d changes almost undistinguishable and a T increase ca. 10°C for each sample. The friction force graphs are shown in **Figs. 5–6** for the tests without lubricator, and in **Figs. 7–8** with lubricating liquid specified in the previous section.

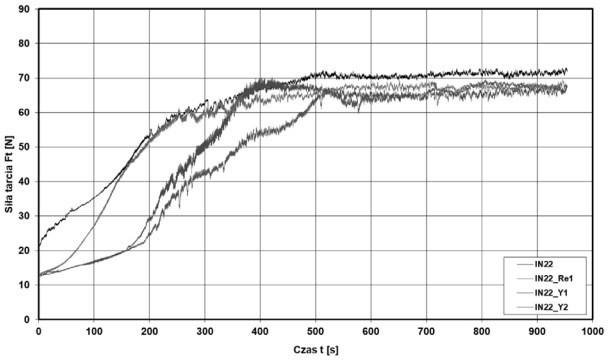

Fig. 5. Graphs of the friction without lubricant for IN22 ceramics/ŁH15 steel (IN22 – unimplanted, Re1 – 1×10^{17} ion/cm^2; Y1 – 1×10^{17} ion/cm^2; Y2 – 2×10^{17} ion/cm^2)

Rys. 5. Przebieg siły tarcia w skojarzeniu ceramika IN22/stal ŁH15 w warunkach tarcia suchego (IN22 – nieimplantowana, Re1 – 1×10^{17} jon/cm^2; Y1 – 1×10^{17} jon/cm^2; Y2 – 2×10^{17} jon/cm^2)

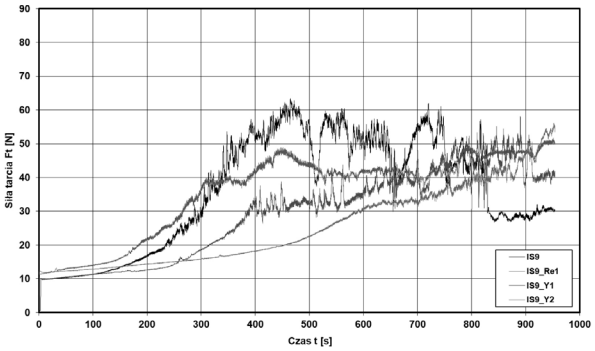

Fig. 6. Graphs of the friction without lubricant for IS9 ceramics/ŁH15 steel (IS9 – unimplanted, Re1 – 1×10^{17} ion/cm^2; Y1 – 1×10^{17} ion/cm^2; Y2 – 2×10^{17} ion/cm^2)

Rys. 6. Przebieg siły tarcia w skojarzeniu ceramika IS9 /stal ŁH15 w warunkach tarcia suchego (IS9 – nieimplantowana, Re1 – 1×10^{17} jon/cm^2; Y1 – 1×10^{17} jon/cm^2; Y2 – 2×10^{17} jon/cm^2)

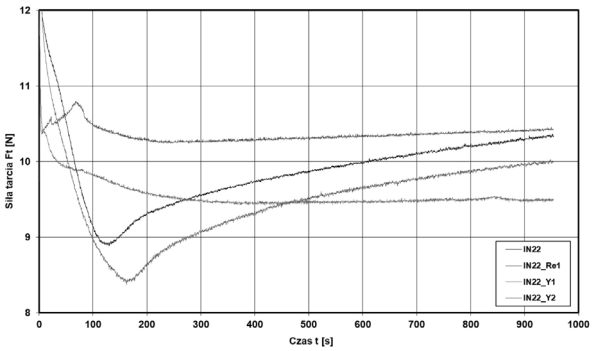

Fig. 7. Graphs of the friction with lubricant for IN22 ceramics/ŁH15 steel (IN22 – unimplanted, Re1 – 1×10^{17} ion/cm^2; Y1 – 1×10^{17} ion/cm^2; Y2 – 2×10^{17} ion/cm^2)

Rys. 7. Przebieg siły tarcia w skojarzeniu ceramika IN22/ stal ŁH15 ze smarowaniem (IN22 – nieimplantowana, Re1 – 1×10^{17} jon/cm^2; Y1 – 1×10^{17} jon/cm^2; Y2 – 2×10^{17} jon/cm^2)

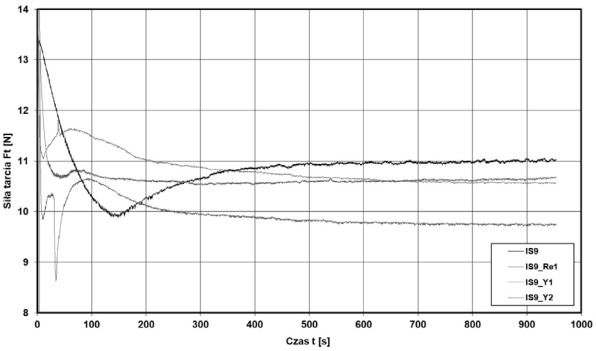

Fig. 8. Graphs of the friction with lubricant for IS9 ceramics/ŁH15 steel (IS9 – unimplanted, Re1 – 1×10^{17} ion/cm^2; Y1 – 1×10^{17} ion/cm^2; Y2 – 2×10^{17} ion/cm^2)

Rys. 8. Przebieg siły tarcia w skojarzeniu ceramika IS9/ stal ŁH15 ze smarowaniem (IS9 – nieimplantowana, Re1 – 1×10^{17} jon/cm^2; Y1 – 1×10^{17} jon/cm^2; Y2 – 2×10^{17} jon/cm^2)

As can be seen in the presented graphs, the rhenium (Re^+) and yttrium (Y^+) ion implantation caused better stability in the friction dynamics, especially in the initial phase of work. The highest instability performed unimplanted IS9 ceramics with oscillations of 10, 20, and even 30 N in the graph in **Fig. 6**. The highest values of friction force $F_t > 70$ N were registered in the case of unimplanted IN22 ceramics without lubrication, **Fig. 5**. On the other hand, the lowest and the most stable friction force between 12 and 40 N revealed IS9 ceramics with yttrium coating (Y^+ 2×10^{17} ion/cm^2) during $t = 800$ s of test. Even though, in some cases, the initial friction force appeared to be higher for implanted surfaces, in general, ion implantation with rhenium (Re^+) and yttrium (Y^+) provided a decrease in friction forces.

A decrease in the friction forces resulted with substantially smaller wear of the implanted surfaces. The inserts after tests underwent qualitative analysis with a laboratory microscope Carl Zeiss JENA with a digital camera HDCE-X5 and software ScopeImage 9.0 (X5). **Figures 9–10** present photographs of worn IN22 inserts with and without coatings after tests without lubricant, and **Figs. 11–12** show respective surfaces of IS9 inserts.

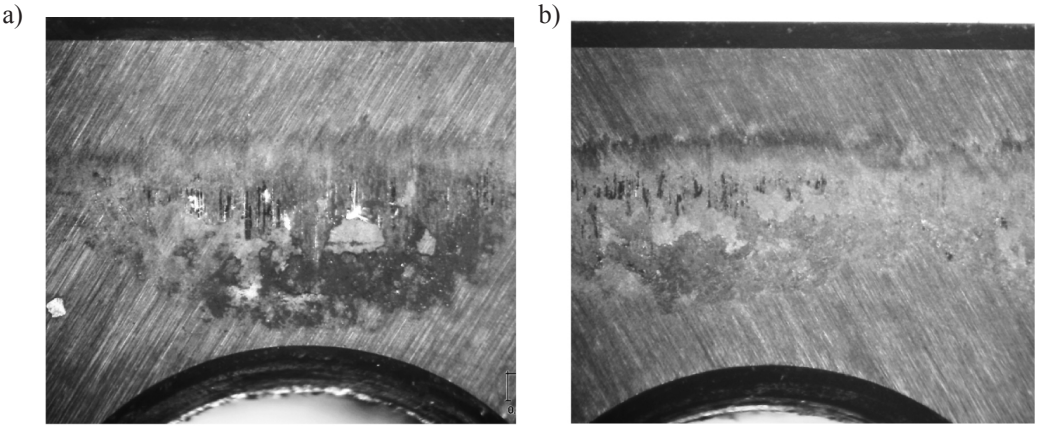

Fig. 9. View of the worn IN22 surface after tests without lubricant: a) unimplanted, b) implanted with Re^+ 1×10^{17} ion/cm^2

Rys. 9. Zużycie powierzchni IN22 po testach bez smarowania: a) nieimplantowana, b) implantowana ionami Re^+ 1×10^{17} ion/cm^2

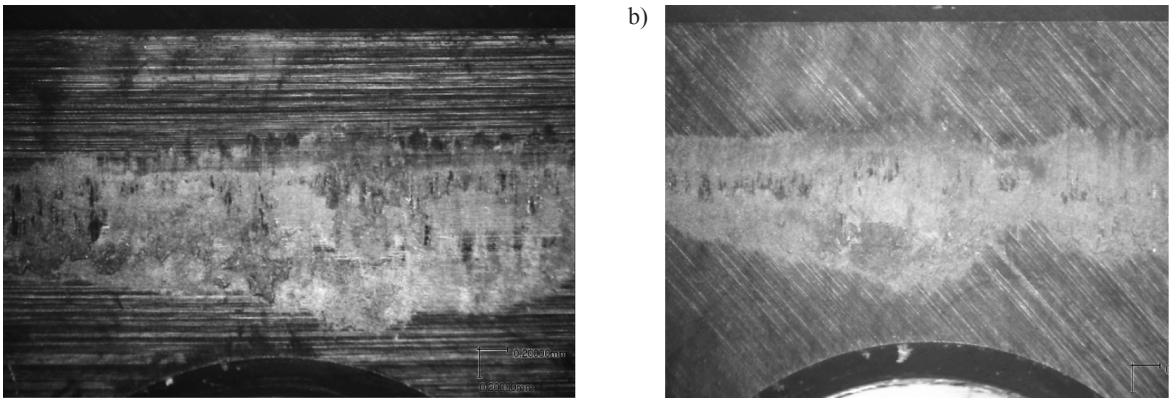

Fig. 10. View of the worn IN22 surface after tests without lubricant implanted with yttrium: a) Y^+ 1×10^{17} ion/cm^2, b) Y^+ 2×10^{17} ion/cm^2

Rys. 10. Zużycie powierzchni IN22 implantowanej jonami itru po testach bez smarowania: a) Y^+ 1×10^{17} jon/cm^2, b) Y^+ 2×10^{17} jon/cm^2

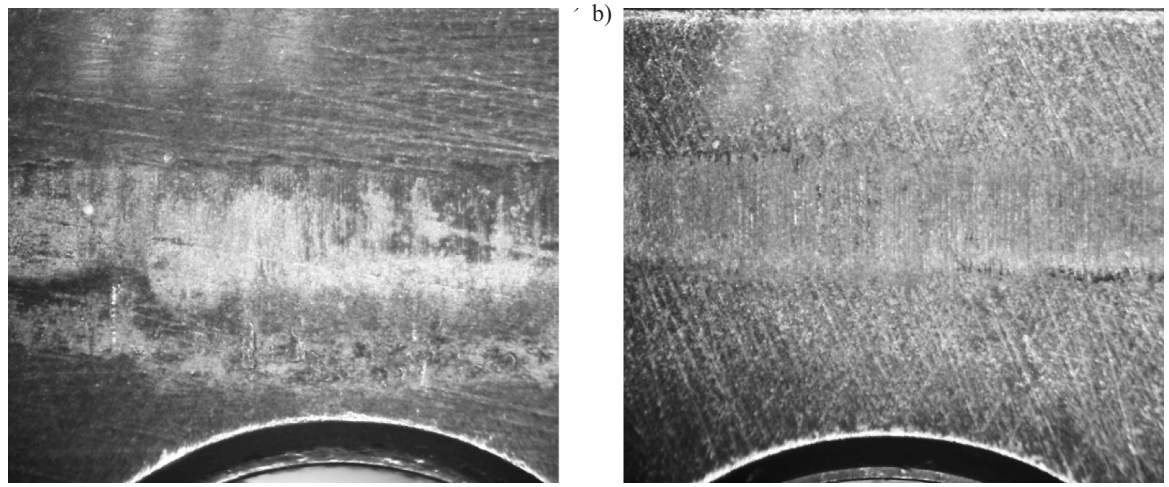

Fig. 11. View of the worn IS9 surface after tests without lubricant: a) unimplanted, b) implanted with Re^+ 1×10^{17} ion/cm^2

Rys. 11. Zużycie powierzchni IS9 po testach bez smarowania: a) nieimplantowana, b) implantowana ionami Re^+ 1×10^{17} ion/cm^2

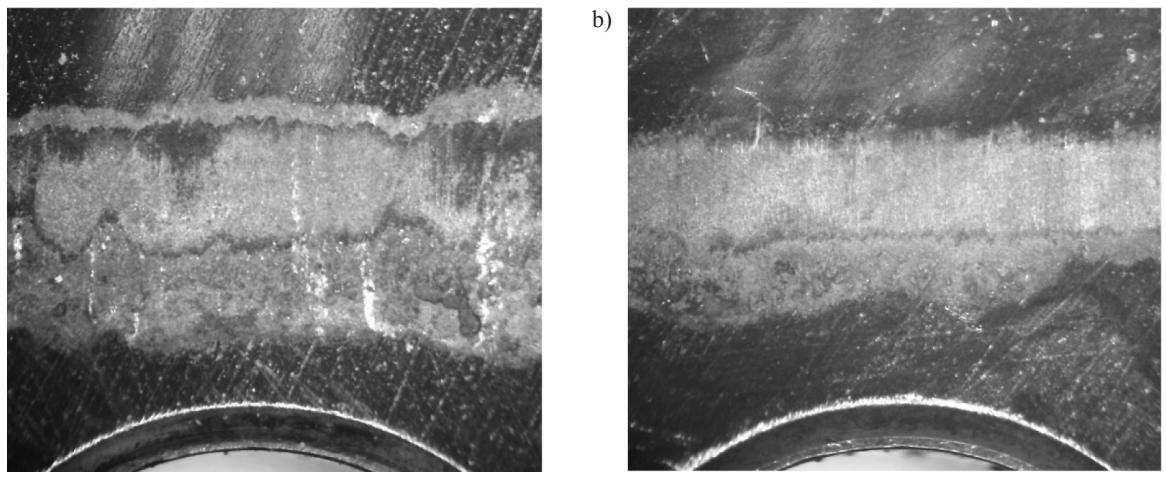

Fig. 12. View of the worn IS9 surface after tests without lubricant implanted with yttrium: a) Y^+ 1×10^{17} ion/cm^2, b) Y^+ 2×10^{17} ion/cm^2

Rys. 12. Zużycie powierzchni IS9 implantowanej jonami itru po testach bez smarowania: a) Y^+ 1×10^{17} jon/cm^2, b) Y^+ 2×10^{17} jon/cm^2

Qualitative analysis of the worn surfaces gives insight into the merits of ion implantation and the complexity of the phenomena and the properties of each material. Therefore, in the case of IN22 ceramics, it can be assumed that both rhenium and yttrium ions improved its wear resistance, since the unimplanted surface revealed the most extensive wear features. It seems also appropriate to assume that rhenium and yttrium ions implanted in a doze of 1×10^{17} ion/cm^2 ensured a quite similar degree of wear protection. A higher doze of Y^+ ions (2×10^{17} ion/cm^2) provided substantially better results with a visibly smaller worn area.

However, the abovementioned observations could not be extended to the IS9 ceramics. Here, a smaller doze of yttrium ions (1×10^{17} ion/cm^2) seemed to have no substantial effect; therefore, that area and the appearance of the worn surface show little difference from the unimplanted material. A doubled doze of Y^+ ions provided substantial improvement, and the worn area appears to be narrower and shallower. However, the rhenium implanted surface looks better in every respect, so it can be assumed that Re^+ implantation provided the best wear resistance of the IS9 ceramics.

Keeping in mind the latest reports on the new ceramic nanostructured composites **[L. 17, 18]**, more investigations are necessary to make further observations on the tribological parameters of various ceramics.

CONCLUSIONS

From the research results, the general conclusion is that cutting performance of TNGA 160408 cutting tools inserts made out of oxide ceramics IN22 as well as nitride ceramics IS9 may be improved by means of ion implantation. Most generally, ions of yttrium and rhenium deposited on the ceramic surfaces with the PVD method improved lubricating properties and the wear resistance of cutting tools. This observation is valid for any application of ceramic parts in mechanical engineering, especially for the highly loaded elements.

More specifically, yttrium ions of a higher implantation dosage substantially decreased friction forces between ceramics and steel and made it more stable. On the other hand, the surface of nitride ceramics implanted with rhenium ions revealed a significantly smaller degree of wear. From the perspective of cutting tools, the former characteristics produce a reduction in the energy consumption of the machining process, while the latter one prolongs the lifetime of an expensive cutting insert.

REFERENCES

1. Tian Ch., Zhou G., Zhang J., Zhang Ch.: Optimization of cutting parameters considering tool wear conditions in low-carbon manufacturing environment. Journal of Cleaner Production, vol. 226, 2019, pp. 706–719.
2. Rech J., Giovenco A., Courbon C., Cabanettes F.: Toward a new tribological approach to predict cutting tool wear. CIRP Annals, vol. 67, No. 1, 2018, pp. 65–68.
3. Kataoka R., Shamoto E.: Influence of vibration in cutting on tool flank wear: Fundamental study by conducting a cutting experiment with forced vibration in the depth-of-cut direction. Precision Engineering, vol. 55, 2019, pp. 322–329.
4. Suárez A., Veiga F., López de Lacalle L.N., Polvorosa R., Wretland A.: An investigation of cutting forces and tool wear in turning of Haynes 282. Journal of Manufacturing Processes, vol. 37, 2019, pp. 529–540.
5. Maruda R.W., Krolczyk G.M., Nieslony P., Wojciechowski S., Michalski M., Legutko S.: The influence of the cooling conditions on the cutting tool wear and the chip formation mechanism. Journal of Manufacturing Processes, vol. 24P1, 2016, pp. 107–115.
6. Vesnovsky O.K.: Ion implantation of cutting tools. Surface and Coatings Technology, vol. 52, No. 3, 1992, pp. 297–299.
7. Poletika M.F., Vesnovsky O.K., Polestchenko K.N.: Ion implantation for cutting tools. Nuclear Instruments and Methods in Physics Research Section B: Beam Interactions with Materials and Atoms, vol. 61, No. 4, 1991, pp. 446–450.
8. Narojczyk J., Morozow D., Narojczyk J.W., Rucki M., Ion implantation of the tool's rake face for machining of the Ti-6Al-4V alloy. Journal of Manufacturing Processes, vol. 34, Part A, 2018, pp. 274–280.
9. Bobzin K.: High-performance coatings for cutting tools. CIRP Journal of Manufacturing Science and Technology, vol. 18, 2017, pp. 1–9.
10. Morozow D., Narojczyk J., Siemiątkowski Z., Rucki M., Zaręba A., Ropelewski Z.: Wear resistance of the cutting tools after yttrium (Y^+) ion implantation. Przegląd Mechaniczny, vol. 77, No. 10, 2018, pp. 22–25.
11. Michalak M., Michalczewski R., Wulczyński J., Szczerek M.: The method of tribotesting of PVD coated elements in oscillatory motion at high temperatures. Tribologia, vol. 259, No. 1, 2015, pp. 77–94.
12. Karpuschewski B., Kundrák J., Varga G., Deszpoth I., Borysenko D.: Determination of specific cutting force components and exponents when applying high feed rates. Procedia CIRP, vol. 77, 2018, pp. 30–33.

13. T-05 Block-on Ring Wear Tester, http://www.katalog.itee.radom.pl/images/stories/karty/58.t-05_ang.pdf (accessed 3.06.2019).
14. Michalczewski R., Piekoszewski W., Szczerek M., Tuszyński W.: A method for tribological testing of thin hard coatings. Tribotest Journal, vol. 9, 2002, pp. 117–130.
15. Łągiewka M., Konopka Z., Zyska A., Nadolski M.: Examining of abrasion resistance of hybrid composites reinforced with SiC and C_{gr} particles. Archives of Foundry Engineering, vol. 8, Special Issue 3, 2008, pp. 59–62.
16. Służałek G., Duda P., Służałek P.: Wizualizacja pomiarów tribologicznych i SGP w programie SolidEdge. X Forum Inżynierskiego ProCAx, Sosnowiec/Siewierz, 6–9 października 2011 r. (in Polish).
17. Gevorkyan E.S., Rucki M., Kagramanyan A.A., Nerubatskiy V.P., Composite material for instrumental applications based on micro powder Al2O3 with additives nano-powder SiC. International Journal of Refractory Metals and Hard Materials, vol. 82, 2019, pp. 336–339.
18. Hong D., Yin Z., Yan Sh, Xu W.: Fine grained Al2O3/SiC composite ceramic tool material prepared by two-step microwave sintering. Ceramics International, vol. 45, No. 9, 2019, pp. 11826–11832.